energies

MDPI

Review

Review of Degradation Models of Battery Energy Storage for Potential Integration into Unit Commitment Problems

Rhianna Maakestad [1,2], Farhan Hyder [2], Gharvin Ramnarase [2] and Bing Yan [2,*]

[1] TRC Companies, Inc., Liverpool, NY 13088, USA; rmaakestad@trccompanies.com
[2] Department of Electrical and Microelectronic Engineering, Rochester Institute of Technology, Rochester, NY 14623, USA; gsr1158@rit.edu (G.R.)
* Correspondence: bxyeee@rit.edu

Abstract

As renewable energy penetration accelerates, battery energy storage systems have become essential for enhancing flexibility, reliability, and economic efficiency in power system operations. For the daily operations of grids, the unit commitment (UC) problem plays a central role in determining the optimized scheduling of generation resources, but current formulations rarely incorporate battery degradation dynamics. The accurate representation of battery aging is crucial, as degradation costs may influence dispatch. This review provides a synthesis of existing approaches for integrating battery degradation into UC formulations. We survey and compare major classes of degradation models and then examine how these models have been embedded into UC frameworks, highlighting trade-offs between modeling accuracy and tractability. This paper concludes with identified research gaps and recommendations for future UC formulations that more faithfully capture battery degradation while maintaining computational efficiency. This review aims to serve as a foundation for researchers and system operators seeking to incorporate realistic battery aging mechanisms into operational decision-making for the evolving low-carbon grid.

Keywords: unit commitment; battery energy storage; battery degradation cost

1. Introduction

Electricity has become an increasingly critical resource in modern society, and the rapid expansion of renewable energy has further elevated the importance of effective grid management. As variable renewable energy sources are integrated into existing power systems, the need for energy storage, particularly Battery Energy Storage Systems (BESSs), continues to grow [1]. BESSs play a key role in mitigating variability, enhancing system flexibility, and supporting reliable grid operation [2–4]. However, their integration also introduces new operational considerations, most notably the need to account for battery degradation within power system operations [5,6]. There are two primary types of degradations for lithium-ion batteries: chemical degradation and mechanical damage [7]. Chemical degradation stems from electrolyte instability, solid electrolyte interphase growth, lithium plating, the oxidation of electrolyte components, the dissolution of electrode materials (particularly manganese), and phase transformations in cathode structures. These are exacerbated by factors such as deep discharge, high charge–discharge currents, extreme temperatures (both low and high), and prolonged high state of charge. Mechanical damage arises from diffusion-induced stress during lithium intercalation/de-intercalation, concentration-dependent elastic stiffening creating internal stress gradients, and external

Check for updates

Received: 31 December 2025
Revised: 11 February 2026
Accepted: 7 March 2026
Published: 12 March 2026

Copyright: © 2026 by the authors. Licensee MDPI, Basel, Switzerland. This article is an open access article distributed under the terms and conditions of the Creative Commons Attribution (CC BY) license.

mechanical loading that impedes lithium-ion diffusion or causes particle fracture and electrical disconnection. As BESSs are integrated into power systems, it is critical to understand how operating conditions including cycle count, depth of discharge, temperature, state of charge windows, charge voltage thresholds, and charge/discharge rates collectively accelerate these degradation pathways, ultimately reducing battery capacity and service life [8].

The two primary optimization problems addressed by grid operators are the unit commitment (UC) problem and the economic dispatch (ED) problem [9]. The UC problem determines which generating units should be online during each time period to meet demand at minimum operating cost while satisfying system-level and unit-level constraints. The solution provides the commitment of generators that is subsequently used by the ED problem, which determines how much power each committed generator should generate during each time period. BESSs can act as both generators (during discharge) and as loads (during charge), offering exceptional operational flexibility for grid operators [10,11]. However, since batteries have a limited lifespan, it is important to consider their degradation or replacement costs while optimizing their operation in the grid. While battery degradation has been incorporated into ED [5], as the degradation can be linked directly to power and energy throughput, it has been far less common in UC. The degradation of lithium-ion batteries (LiBs), which dominate modern grid-scale storage, arises primarily from two mechanisms: calendar aging and cycle aging [12]. Calendar aging refers to capacity loss over time, whereas cycle aging reflects the wear caused by repeated charging and discharging. Key factors such as state of charge (SOC), depth of discharge (DOD), and cycle count significantly influence both degradation rate and overall battery lifetime. Integrating these degradation mechanisms into the UC problem, however, is challenging. UC formulations require degradation costs to be expressed in a tractable and quantifiable manner, yet many aging models are highly nonlinear or rely on detailed electrochemical behaviors that are impractical for large-scale discrete optimization [13]. As a result, researchers have developed a variety of simplified representations [14], such as throughput-based approximations and cycle-counting methods, to capture battery aging in grid operation problems. Such simplifications introduce a fundamental trade-off between physical accuracy and computational efficiency. Throughput-based models are computationally lightweight but neglect critical stress factors, while cycle-counting methods offer greater fidelity at the cost of additional binary variables and increased solution times.

This paper provides a review of existing approaches for modeling battery degradation for potential integration into UC problems. We summarize major degradation modeling paradigms, discuss their suitability for operational studies, and compare their trade-offs. In the literature, battery degradation is simplified to basic variables and parameters that can be integrated into optimization problems. The most common implementation is to represent degradation as a function based on the replacement cost of batteries. Each time a battery reaches the End of Life (EOL), commonly known as 80% of the original capacity of the battery [6,12,15,16], it needs to be replaced [17]. In this way, the cost of battery degradation is directly related to the cost of using the BESS. There are two main types of degradation models: energy throughput models and cycle-counting models. In Section 2, energy throughput is reviewed and a few degradation cost models derived from this approach are presented. In Section 3, cycle-counting is reviewed, the differences between cycle and calendar aging are discussed, and a few representative degradation cost models based on this approach are introduced. In Section 4, current limitations are highlighted and promising research directions for developing UC models that more accurately and efficiently represent BESS aging within the evolving low-carbon power grid are outlined.

2. Review and Analysis of Energy Throughput Models

Energy throughput models are based on a simplistic theory: a battery degrades proportionally to the amount of energy that moves through it [14]. Because of its exceptional computational efficiency, the energy throughput model is often the preferred choice for representing battery degradation in power system studies and has been widely applied in battery integration research [6,17,18]. The first type of model [17] is shown in Equation (1).

$$c^{dis} = \alpha^{fit} \frac{Cell\ replace\ cost}{DOD\ operation\ range} \quad (1)$$

In this model, the marginal discharging cost (c^{dis}) of the battery is determined by allocating the cell replacement cost over the battery's cycle life degradation profile. Equation (1) uses a linear fit of the slope of depth of discharge vs. capacity loss per cycle curve, as shown in Figure 1. The data used in Figure 1 was obtained by performing a dynamic stress test (DST) on lithium manganese oxide (LMO) batteries [12]. Experimental data for the empirical models was collected using climatic chambers to maintain controlled temperatures and isolate stress factors like SOC during calendar aging tests, while battery cyclers applied repetitive charge–discharge profiles to measure capacity fade under varying DOD conditions. Impedance spectroscopy and on-site diagnostics were additionally employed to track cell resistance increases and update battery life estimates, capturing degradation mechanisms beyond simple capacity loss. This linear fit is represented by α^{fit}, which is used as a scalar that defines how the depth of discharge modifies the cell replacement cost. The ratio of α^{fit} to the operating depth of discharge range effectively adjusts the cell replacement cost to be more representative of realistic battery degradation. The DOD operating range is defined as 20% to 90% SOC, which prevents deep discharge and maintains the validity of the linear fit model. A similar model was reported in a recent study [19]. However, in this approach, instead of using a linear fit term in Equation (1), the authors incorporate the maximum possible energy throughput until the EOL of the battery in the denominator, calculated from a non-linear battery aging model. In addition, the battery investment cost is used in place of the cell replacement cost to capture the costs at the start of the battery life cycle instead of the end. The modeling of energy throughput across both studies [17,19] is comparable.

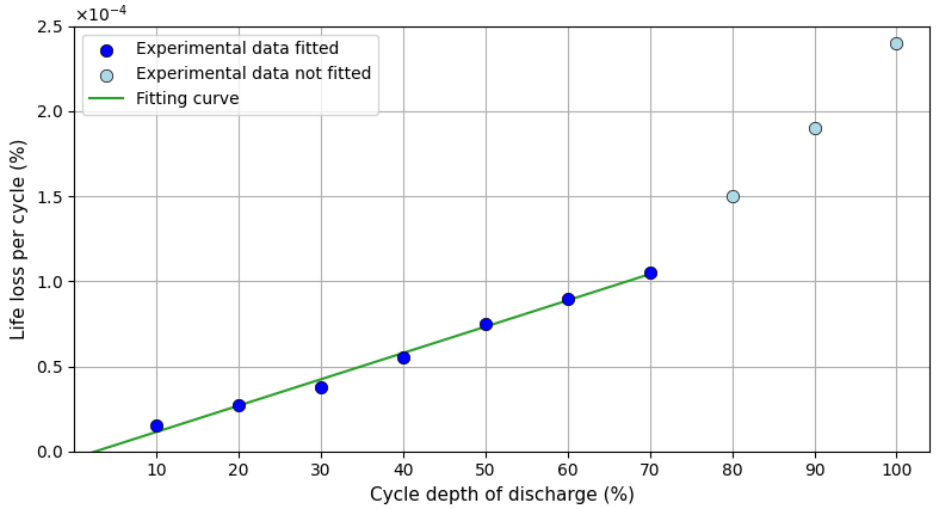


Figure 1. Depth of discharge [%] vs. loss of capacity per cycle [%] plot used to derive the α^{fit} term in Equation (1). Adapted from [17].

This type of model incorporates the DOD as the main factor in degradation costs [17,19]. The reason the DOD is critical to battery degradation is that the larger the

DOD, the more severe the degradation becomes. This effect is not consistent across all LiBs: lithium iron phosphate (LFP) batteries are less sensitive to DOD, meanwhile Lithium Nickel Cobalt Aluminum (NCA) and Lithium Nickel Manganese Cobalt (NMC) batteries are significantly more sensitive to the DOD. This is commonly attributed to the differences in the anodes, meaning that the DOD has a measurable effect on the degradation of the anode [15].

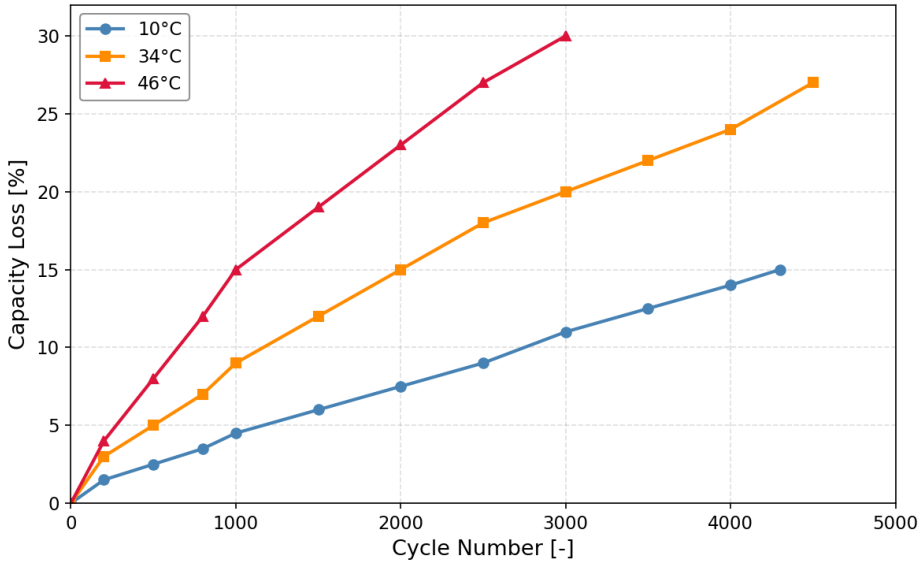
The second type of model, based on the energy throughput theory, utilizes a battery degradation penalty cost ($\$/MWh$) and remaining battery capacity [6]. The remaining battery capacity ($Q_{rem}(t)$) is expressed as a fraction of the initial battery capacity (Q_B) in time period t. In [6], the battery degradation cost is estimated using two approaches. The first approach, based on the degradation models developed in [13], is shown in Equation (2). Here, the degradation penalty cost per time period ($\Delta c(t)$) is equal to the current discharge power ($P^{dh}(t)$) multiplied by the penalty cost ($C_{penalty}$) and weighted by the battery fade constant (f_B) and the remaining battery capacity ($Q_{rem}(t) = 1 - EOL$). The battery fade constant (f_B) is analogous to the α^{fit} from [17]. The value of f_B is adversely affected by the operating temperature of the battery and the DOD. Figure 2a shows capacity loss as a function of cycle number for a 0.5 C charge rate at three operating temperatures (10 °C, 34 °C, and 46 °C) and Figure 2b shows capacity loss as a function of cycle number for varying depths of discharge (20–100% DOD), with scatter points representing measured data and lines representing model fits [20]. Similar work was also reported in [21], where the investment cost was used instead of a penalty cost $C_{penalty}$. However, [6] argues that several additional factors must be considered for determining the penalty cost, where investment cost alone might not be sufficient.

$$\Delta c(t) = f_B \cdot P^{dh}(t) \cdot \frac{C_{penalty}}{1 - EOL} \tag{2}$$

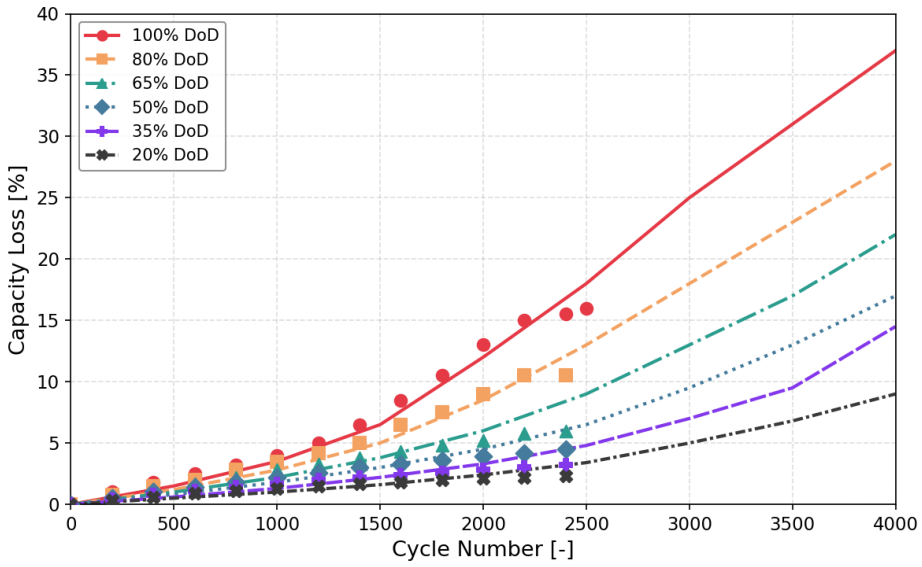
The second approach reported in [6] incorporates the DOD range using SOC in addition to the characteristics already captured in Equation (2). This model is implemented as a reference to a different explicit series of tests completed in [22], where it is proved that by limiting the SOC range, the effect of battery degradation could be translated into a simple linear function. The specific SOC range used in [22] is SOC_{min} = 10% to SOC_{max} = 70%. Building upon the work done by [22], a model with usable SOC adjusted to SOC_{min} = 30% and SOC_{max} = 90% for all t was developed in [6], as shown in Equation (3). The incorporation of a reduced SOC range increases the battery's life cycle. Additionally, it ensures that the model can assume no battery fade until the degradation of the battery's usable capacity.

$$\Delta c(t) = f_B \cdot \frac{P^{dh}(t)}{SOC_{max} - SOC_{min}} \cdot \frac{C_{penalty}}{1 - EOL} \tag{3}$$

The reason this type of model is possible is that battery degradation depends on both the range of use (DOD) and the average level of charge (SOC) during cycling. DOD is defined as the difference between the maximum and minimum SOC used in a system (e.g., cycling between 10% and 60% SOC gives a DOD of 50%). However, battery lifetime depends on more than just the DOD; where the SOC range is centered is also critical. For example, the two ranges 10–60% SOC and 25–75% SOC both have a DOD of 50%, but 10–60% SOC is centered on 35% SOC and 25–75% SOC is centered on 50% SOC. Research by Ecker et al. [16] has shown that the center point of this range has a major impact, with an optimal center around 50% SOC. Therefore, two cycles with the same DOD can have different effects on the battery based on their average SOC.



(**a**)



(**b**)

Figure 2. Capacity loss [%] vs. cycle number curve. (**a**) Impact of temperature on degradation. (**b**) Impact of DOD on degradation. Adapted from [20].

It is worth examining whether energy throughput models oversimplify cycle aging. By assuming degradation is linearly proportional to energy throughput, these models treat all MWh as equally costly. However, lithium-ion batteries degrade via nonlinear, stress-driven mechanisms where deep cycles cause disproportionately greater wear than shallow cycles per unit energy. This structural misspecification systematically under-costs deep cycling applications (e.g., arbitrage) while over-costing shallow cycling services (e.g., frequency regulation), creating perverse dispatch incentives opposite to wear-minimizing operation.

In summary, the energy throughput models highlight the importance of the DOD and SOC range to the lifetime expectancy of a battery. However, these models do not capture the day-to-day cycling of the batteries and oversimplify cycle aging, which significantly affects battery degradation.

3. Review and Analysis of Cycle-Counting Models

Cycle-based degradation models are derived from the principle that batteries age according to the characteristics of individual charge–discharge cycles rather than the total amount of energy processed. In contrast to energy throughput models, which assume degradation is proportional to cumulative energy flow, cycle-based approaches explicitly account for the amplitude (i.e., DOD), mean SOC, temperature, and duration of each cycle.

A representative example of this modeling is the semi-empirical framework in [12], where the total linearized degradation is decomposed into cycle aging and calendar aging [23–27]. Calendar aging describes the natural, time-dependent degradation of a battery cell even when it is not being actively cycled and is primarily driven by storage conditions such as average SOC and temperature. Calendar aging (L_{cal}) over a period of time (t) is a function of average SOC (represented by $\bar{\sigma}$) and the average cell temperature ($\bar{T}_c$) as shown in Equation (4) below.

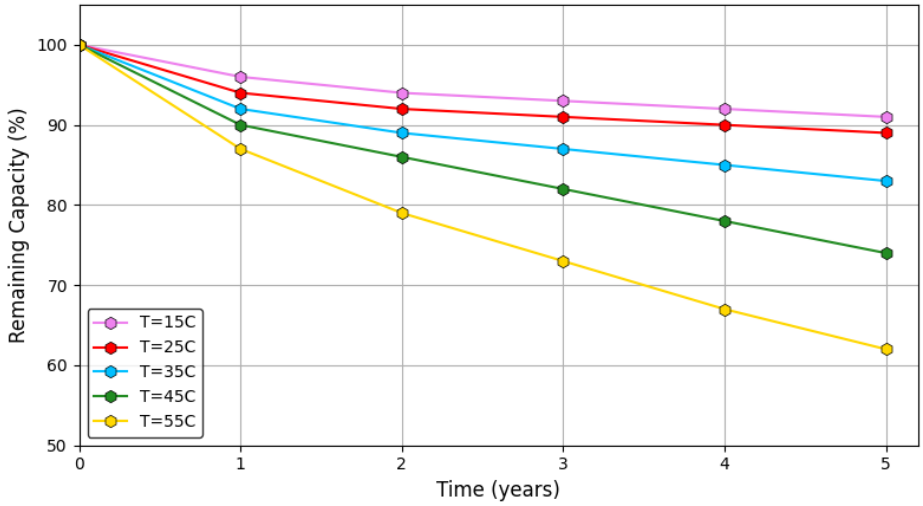
$$L_{cal} = f_t(t, \bar{\sigma}, \bar{T}_c) \tag{4}$$

Figure 3a shows the remaining capacity over time for several temperature conditions ranging from 15 °C to 55 °C. The curves clearly demonstrate the strong influence of temperature on degradation: batteries operated at higher temperatures exhibit a much faster decline in remaining capacity. Figure 3b presents capacity fade for different average SOC between 60% and 100%, where degradation is faster at higher SOC levels within this range. The curves in (b) lie closer together than those in (a), indicating that the effect of average SOC on degradation is smaller than the impact of temperature. To further illustrate the impact of temperature on battery degradation, consider the following example from [28]. In this study examining Lithium Iron Phosphate (LFP) cells, capacity fade was tracked over continuous cycling at 25 °C and 55 °C. At 25 °C, representative of nominal room temperature, the cell exhibited an initial capacity fade rate of approximately 0.35% per day, which gradually declined to 0.05% per day after nearly 700 days of operation. By contrast, at 55 °C, a temperature indicative of an unconditioned enclosure during summer conditions, the cell sustained only 130 days of continuous cycling, with a terminal capacity fade rate of approximately 0.20% per day. This corresponds to an approximate 80% reduction in operational lifetime under elevated thermal stress. Such quantitative bounds provide clear justification for including temperature as a first-order degradation factor in simplified, computationally tractable UC formulations, particularly for systems deployed in regions or enclosures without active thermal regulation.

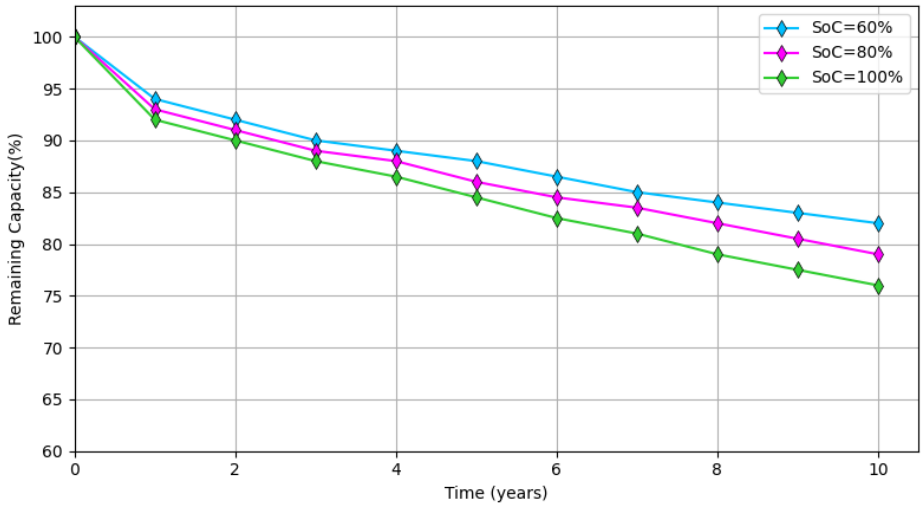
Cycle aging, in contrast, represents the additional degradation incurred each time the battery is charged and discharged. Cycle aging depends not only on the number of cycles but also on how much energy each cycle processes and under what conditions it is processed. Cycle aging (L_{cyc}) is a function of the DOD (δ_i), cycle SOC (σ_i), full or half cycle (n_i), and the cell temperature ($T_{c,i}$) for each individual cycle (i) of the cell (c). The accumulated cycle aging over N cycles is shown in Equation (5).

$$L_{cyc} = \sum_{i}^{N} n_i f_c(\sigma_i, \delta_{i,} T_{c,i}) \tag{5}$$

The distinction between full and half cycles is determined using the rainflow cycle-counting algorithm [12]. Given a user-provided SOC time series, the rainflow method extracts individual cycles, identifies their amplitudes and mean values, and classifies them as full or half cycles. In this way, the algorithm converts an arbitrary SOC profile into the set of cycle parameters needed for degradation evaluation.



(**a**)



(**b**)

Figure 3. Impacts of temperature and average SOC on calendar aging. (**a**) Calendar aging with varying temperature at 50% SOC. (**b**) Calendar aging with varying SOC at 25 °C. Adapted from [12].

To more accurately capture the nonlinear DOD sensitivity observed in cycle life tests, an empirical DOD stress function for lithium-ion manganese oxide (LMO) batteries was developed in [12], which offers a better fit than previously used exponential or quadratic models. This formulation reflects the sharply increasing marginal damage associated with deeper cycles, a key driver of lithium-ion aging. The inherent nonlinearity of degradation and rapid initial capacity loss from solid electrolyte interphase (SEI) formation, followed by slower mid-life fade, is modeled through a two-exponential mapping between linearized stress accumulation and actual capacity loss, enabling the reproduction of both the early fast-aging phase and the accelerated end-of-life behavior. Cycle identification is performed using the rainflow counting algorithm, which extracts the DOD, mean SOC, and duration of each cycle from the SOC trajectory. This allows the model to evaluate degradation under irregular cycling patterns such as frequency regulation, arbitrage, or other optimization-driven dispatch signals.

Although the nonlinear SEI mapping and rainflow counting cannot be embedded directly into mixed-integer unit commitment formulations, the model is well suited for deriving marginal degradation cost coefficients. By simulating representative operation

patterns, applying rainflow cycle identification, and evaluating per-cycle life loss, the effective degradation costs can be computed for shallow, moderate, and deep cycles. These costs can then be represented as linear or piecewise linear terms in the UC objective function, enabling cycle-dependent, chemistry-specific degradation behavior to be captured in a tractable manner.

To bridge the gap between physical accuracy and optimization requirements, a reduced-order model was developed in [29], where the nonlinear dependence of degradation on DOD is retained while eliminating the history dependence inherent in rainflow counting. To represent the incremental life loss caused by a cycle of depth (δ), an empirical life cycle stress function $\Phi(\delta)$ is derived by conducting stress tests on NMC batteries. Then the DOD interval $[0, 1]$ is partitioned into J equal-depth segments, and the marginal cost associated with segment j is computed as shown in Equation (6), where E_{rate} is the energy capacity of the battery.

$$c_j = \frac{R}{\eta_{\text{dis}} E_{\text{rate}}} J \left[\Phi\left(\frac{j}{J}\right) - \Phi\left(\frac{j-1}{J}\right) \right]. \tag{6}$$

This formulation spreads the replacement cost (R) across the incremental life loss predicted by the empirical stress function, yielding a convex set of marginal costs that increases with cycle depth. Battery energy is tracked in J depth layers, and the optimization determines how much discharge power to draw from each layer. Because deeper layers impose higher costs, the model naturally favors shallow cycling, consistent with physical degradation patterns. The total degradation cost becomes

$$C_{\text{deg}} = \sum_{t,j} c_j \, p_{t,j}^{\text{dis}}, \tag{7}$$

which is a fully linear expression that can be inserted directly into UC objectives. It is further proven that as $J \to \infty$, the linear approximation converges to the true rainflow-based degradation estimate. According to [29], a total of 16 segments is sufficient to make the error negligible. A similar strategy for integrating cycle aging effects into operational scheduling is presented in [30], where a stochastic framework explicitly incorporates DOD-dependent degradation costs for batteries in microgrids.

These two modeling approaches [12,29] illustrate the tension between fidelity and tractability in battery degradation modeling. The cell-level empirical model [12] provides a detailed understanding of aging mechanisms and accurately captures nonlinearities associated with DOD and SOC, but its dependence on cycle extraction and nonlinear stress functions prevents direct integration into UC. In contrast, the piecewise linear model from [29] preserves the essential DOD-driven behavior while producing a convex, linear cost structure that aligns with the computational requirements of UC. As a result, it represents a practical pathway for incorporating physically meaningful degradation dynamics into system-level optimization.

Another model towards embedding degradation directly into optimization is provided by the differentiable, DOD-driven framework introduced in [31]. This approach converts the manufacturer-supplied cycle life curve into a one-cycle marginal degradation cost $C_E(\text{DOD})$, which is then evaluated through an auxiliary SOC trajectory designed to emulate rainflow cycle boundaries without requiring discrete logic or binary cycle start variables. By forcing the auxiliary SOC to mirror the actual SOC during discharge and lag during charging periods, the model implicitly identifies cycle turning points, enabling a smooth, decision-dependent estimate of cycle depth that is compatible with both nonlinear programming and piecewise linear Mixed-Integer Linear Programming (MILP) formulations. A similar DOD-based model is developed in [32], where cycle aging is modeled

within an MILP framework using a depth-of-discharge-dependent cost function. In this formulation, degradation is translated into a piecewise linear life loss curve obtained from rainflow-based pre-processing, enabling direct integration into day-ahead economic dispatch and reserve scheduling. Both models yield a computationally lightweight degradation representation that scales efficiently to large system studies. However, they attain tractability by reducing the aging process to a single dominant variable (DOD) while omitting or implicitly aggregating other influential stress factors such as C-rate, average SOC, temperature, and SEI layer dynamics. As a result, although well suited for real-time scheduling and market participation studies, the framework provides limited fidelity under operating conditions characterized by aggressive cycling, fast charging and discharging ramps, or the irregular dispatch trajectories typically induced by UC decisions. Additionally, it has been reported that temperature and discharge C-rate are relatively more influential stress factors than charge C-rate [33].

A more comprehensive integration of degradation into optimization has been enabled by a logarithmic reformulation introduced in [34]. In this approach, the multiplicative stress factors governing both calendar and cyclic aging are transformed into a separable additive expression in the log domain, which can then be linearized through a Constraint Cost Variable (CCV) representation. This transformation preserves the essential physics of degradation while avoiding the need for additional binary variables, thereby maintaining computational tractability within MILP-based frameworks. Furthermore, a real-time, decision-dependent cycle-counting mechanism is incorporated to emulate the rainflow counting algorithm using concavity changes in the SOC trajectory—an innovation that enables cycle identification directly inside the optimization rather than through post-processing. When combined, these developments allow a high-fidelity, multi-factor degradation model to be embedded directly within UC and dispatch formulations, rather than being restricted to offline evaluation. As a result, degradation-aware UC becomes capable of capturing the electrochemical drivers of long-term battery wear with a level of accuracy that was previously unattainable in MILP-based system operations. However, the fidelity of the linearized model depends on the quality and and density of the CCV breakpoints and can weaken when stress factor interactions become strongly nonlinear.

4. Discussion and Insights

To consolidate the preceding review and highlight the essential distinctions between the two modeling paradigms, Table 1 provides a multi-criteria comparison of energy throughput and cycle-counting approaches. This comparison illustrates the fundamental accuracy–tractability trade-off and serves as a reference for selecting degradation representations in UC studies.

Table 1. Comparison of battery degradation modeling approaches for unit commitment integration.

Criteria	Energy Throughput Models [6,12,13,16–21]	Cycle-Counting Models [22–34]
Core Principle	Degradation is proportional to cumulative energy processed	Degradation depends on individual cycle characteristics (DOD, SOC, temperature)
Key Parameters	DOD, SOC range, replacement cost, energy throughput	DOD, mean SOC, temperature, replacement cost, cycle count, full/half cycles

Table 1. *Cont.*

Criteria	Energy Throughput Models [6,12,13,16–21]	Cycle-Counting Models [22–34]
Physical Fidelity	Low to moderate: aggregates wear, ignores cycle depth distribution	High: captures DOD nonlinearity, SOC-cycle parameters, calendar aging
Computational Tractability	High: linear or convex, minimal binary variables	Low to moderate: requires rainflow model preprocessing or reformulation
Data Requirements	Low: manufacturer cycle life curves, replacement cost	High: detailed aging test data, temperature/SOC stress functions
UC Integration Suitability	Direct, mature, widely implemented	Indirect or via linearization; emerging MILP-compatible formulations
Strengths	Simple, fast, easy to parameterize, suitable for large systems	Captures realistic aging dynamics, chemistry-specific, decision-dependent
Limitations	Ignores cycle-by-cycle variation; may over/underestimate wear	Computationally intensive; rainflow-based non-linear; parameter-sensitive
Representative Equations	Equations (1)–(3)	Equations (4)–(7)

Note: DOD = Depth of Discharge; SOC = State of Charge; UC = Unit Commitment; MILP = Mixed-Integer Linear Programming.

Despite the advancements offered by the degradation models reviewed in Sections 2 and 3, several challenges remain when these models are incorporated into a UC framework. These challenges arise primarily from the characteristics of battery aging and the structural properties of UC formulations.

1. Nonlinearity and Computational Complexity: Battery degradation is characterized by nonlinear and chemistry-specific behaviors. As shown in the empirical relationships of DOD, SOC, temperature, and cycle life, degradation mechanisms are inherently nonlinear and often nonconvex. UC problems, however, are predominantly solved using MILP formulations to ensure tractability within operational time limits. Incorporating nonlinear degradation terms, therefore, requires linearization or approximation, which can either oversimplify the physics or significantly increase model size. In addition, computational complexity is increased when degradation is included. Additional variables such as remaining capacity, stress factors, accumulated wear, number of cycles, or SOC-dependent coefficients expand the dimensionality of the UC problem. More detailed models require capturing multiple interacting stress factors, further increasing the computational burden and potentially challenging real-time or day-ahead operational timelines.
2. Parameter Sensitivity and Uncertainty: Degradation parameters are highly sensitive to battery chemistry, temperature, SOC range, and experimental conditions. These parameters vary significantly across manufacturers and operational settings, meaning that degradation-aware UC solutions may be sensitive to mis-specified or uncertain model parameters. Underestimation may accelerate battery wear, while overestimation may discourage the economically optimal use of storage assets.
3. Temporal Mismatch Between UC and Battery Aging: The mismatch between UC's short-term operational horizon and the long-term nature of battery degradation introduces conceptual challenges. UC is typically solved over a 24 to 36 h horizon, whereas battery aging occurs over months or years. Mapping short-term dispatch decisions onto long-term wear requires assumptions about the amortization of degradation

cost, yet these assumptions may not fully capture interactions between long-term degradation trajectories and short-term operational behavior.

4. Lack of Standardization and Market Alignment: There is currently no industry consensus or standardized regulatory approach for incorporating degradation costs into UC formulations. Market rules in most regions do not explicitly compensate for degradation-aware operation, and system operators vary in how degradation is treated operationally. This lack of standardization limits adoption and challenges the development of universally applicable degradation-aware UC models.

To overcome the above challenges, future research may focus on developing advanced linearization and reformulation techniques that preserve the nonlinear nature of battery aging while remaining compatible with MILP-based UC models; creating robust and uncertainty-aware frameworks to address parameter sensitivity; bridging timescales between short-term UC and long-term degradation through hierarchical or model predictive control approaches; designing standardized degradation pricing mechanisms; improving real-time cycle-counting; integrating physics-based and data-driven degradation models; enabling multi-service degradation co-optimization; and scaling UC algorithms for large storage fleets. Together, these directions aim to close the gap between electrochemical realism and operational feasibility in degradation-aware unit commitment.

5. Conclusions

This review has examined existing approaches for modeling battery degradation within the context of the UC problem. It summarizes both energy throughput and cycle-counting frameworks and evaluates their suitability for operational decision-making in modern power systems. Energy throughput models provide computationally simple representations that relate degradation to cumulative energy processed, while cycle-counting models offer increased physical realism by accounting for DOD, SOC, temperature, and stress-dependent aging behaviors. However, each category presents trade-offs between accuracy, data requirements, and computational tractability.

Although several degradation models can be embedded into UC formulations, significant challenges remain in practice. Degradation mechanisms are highly nonlinear, model parameters are sensitive to chemistry and operating conditions, and the temporal mismatch between the short-term UC horizon and long-term battery aging complicates the interpretation of degradation costs. The modeling choices require careful trade-offs between capturing dominant stress factors and maintaining tractability for day-ahead scheduling. Overly simplified models risk underestimating wear and accelerating asset degradation, while overly complex models may overestimate degradation costs and discourage economically optimal battery use. Ultimately, the selection of an appropriate degradation representation depends on the specific battery chemistry, operational context, and acceptable computational burden. In addition, a lack of standardized market rules and modeling conventions limits the widespread adoption of degradation-aware UC formulations across system operators.

The integration of battery degradation into UC is both necessary and complex. As battery energy storage systems continue to expand their role in balancing variable renewable generation, there is a growing need for UC models that can represent degradation in a way that is both computationally efficient and physically meaningful. Future research should focus on developing simplified yet accurate degradation approximations, creating scalable optimization techniques, and exploring uncertainty-aware formulations that better capture the interactions between operational decisions and long-term battery health. Continued progress in these areas will support more economically efficient, reliable, and sustainable grid operations as the power system transitions toward higher renewable penetration.

https://doi.org/10.3390/en19061425

Author Contributions: Conceptualization, R.M.; methodology, R.M., F.H. and G.R.; validation, R.M. and G.R.; supervision, B.Y.; project administration, B.Y.; writing—original draft preparation, R.M. and F.H.; writing—review and editing, F.H. and B.Y.; visualization, R.M. and F.H. All authors have read and agreed to the published version of the manuscript.

Funding: This work is supported in part by the National Science Foundation (NSF) under grant ECCS-2340095. Any opinions, findings, conclusions, or recommendations expressed in this material are those of the authors and do not necessarily reflect the views of the NSF.

Data Availability Statement: No new data were created or analyzed in this study.

Conflicts of Interest: Author Rhianna Maakestad is employed by the company TRC Companies, Inc. The remaining authors declare that the research was conducted in the absence of any commercial or financial relationships that could be construed as a potential conflict of interest.

References

1. California Independent System Operator (CAISO). 2023 Special Report on Battery Storage. 2023. Available online: https://www.caiso.com/documents/2023-special-report-on-battery-storage-jul-16-2024.pdf (accessed on 27 December 2025).
2. Habibi, M.; Vahidinasab, V.; Aghaei, J.; Mohammadi-Ivatloo, B. Assessment of energy storage systems as a reserve provider in stochastic network constrained unit commitment. *IET Smart Grid* **2021**, *4*, 139–150. [CrossRef]
3. Park, H.; Kim, M. Expected Benefits of Coordinated Energy Storage Operation in Stochastic Unit Commitment with Enhanced Deliverability of Reserves. *IEEE Access* **2024**, *12*, 18280–18294. [CrossRef]
4. Moreira, A.; Fanzeres, B.; Silva, P.; Heleno, M.; Marcato, A.L.M. On the role of Battery Energy Storage Systems in the day-ahead Contingency-Constrained Unit Commitment problem under renewable penetration. *Electr. Power Syst. Res.* **2024**, *235*, 110856. [CrossRef]
5. Schade, C.; Egging-Bratseth, R. Battery degradation: Impact on economic dispatch. *Energy Storage* **2024**, *6*, e588. [CrossRef]
6. Wankmüller, F.; Thimmapuram, P.R.; Gallagher, K.G.; Botterud, A. Impact of battery degradation on energy arbitrage revenue of grid-level energy storage. *J. Energy Storage* **2017**, *10*, 56–66. [CrossRef]
7. Shchurov, N.I.; Dedov, S.I.; Malozyomov, B.V.; Shtang, A.A.; Martyushev, N.V.; Klyuev, R.V.; Andriashin, S.N. Degradation of lithium-ion batteries in an electric transport complex. *Energies* **2021**, *14*, 8072. [CrossRef]
8. Manoharan, P.; Chandrasekaran, K.; Chandran, R.; Ravichandran, S.; Mohammad, S.; Jangir, P. An effective strategy for unit commitment of microgrid power systems integrated with renewable energy sources including effects of battery degradation and uncertainties. *Environ. Sci. Pollut. Res.* **2024**, *31*, 11037–11080. [CrossRef]
9. Wood, A.J.; Wollenberg, B.F.; Sheblé, G.B. *Power Generation, Operation, and Control*; John Wiley & Sons: Hoboken, NJ, USA, 2013.
10. Pozo, D.; Contreras, J.; Sauma, E.E. Unit commitment with ideal and generic energy storage units. *IEEE Trans. Power Syst.* **2014**, *29*, 2974–2984. [CrossRef]
11. Chen, Y.; Baldick, R. Battery storage formulation and impact on day ahead security constrained unit commitment. *IEEE Trans. Power Syst.* **2022**, *37*, 3995–4005. [CrossRef]
12. Xu, B.; Oudalov, A.; Ulbig, A.; Andersson, G.; Kirschen, D.S. Modeling of Lithium-Ion Battery Degradation for Cell Life Assessment. *IEEE Trans. Smart Grid* **2018**, *9*, 1131–1140. [CrossRef]
13. Peterson, S.B.; Apt, J.; Whitacre, J. Lithium-ion battery cell degradation resulting from realistic vehicle and vehicle-to-grid utilization. *J. Power Sources* **2010**, *195*, 2385–2392. [CrossRef]
14. Xu, B. The role of modeling battery degradation in bulk power system optimizations. *MRS Energy Sustain.* **2022**, *9*, 198–211. [CrossRef]
15. Preger, Y.; Barkholtz, H.M.; Fresquez, A.; Campbell, D.L.; Juba, B.W.; Romàn-Kustas, J.; Ferreira, S.R.; Chalamala, B. Degradation of Commercial Lithium-Ion Cells as a Function of Chemistry and Cycling Conditions. *J. Electrochem. Soc.* **2020**, *167*, 120532. [CrossRef]
16. Ecker, M.; Nieto, N.; Käbitz, S.; Schmalstieg, J.; Blanke, H.; Warnecke, A.; Sauer, D.U. Calendar and cycle life study of Li(NiMnCo)O2-based 18650 lithium-ion batteries. *J. Power Sources* **2014**, *248*, 839–851. [CrossRef]
17. Xu, B.; Wang, Y.; Dvorkin, Y.; Fernandez-Blanco, R.; Silva-Monroy, C.A.; Watson, J.P.; Kirschen, D.S. Scalable Planning for Energy Storage in Energy and Reserve Markets. *IEEE Trans. Power Syst.* **2017**, *32*, 4515–4527. [CrossRef]
18. Zia, M.F.; Elbouchikhi, E.; Benbouzid, M. Optimal operational planning of scalable DC microgrid with demand response, islanding, and battery degradation cost considerations. *Appl. Energy* **2019**, *237*, 695–707. [CrossRef]
19. Preis, V.; Biedenbach, F. Assessing the incorporation of battery degradation in vehicle-to-grid optimization models. *Energy Inform.* **2023**, *6*, 33. [CrossRef]

20. Vermeer, W.; Mouli, G.R.C.; Bauer, P. A comprehensive review on the characteristics and modeling of lithium-ion battery aging. *IEEE Trans. Transp. Electrif.* **2021**, *8*, 2205–2232. [CrossRef]
21. Ortega-Vazquez, M.A. Optimal scheduling of electric vehicle charging and vehicle-to-grid services at household level including battery degradation and price uncertainty. *IET Gener. Transm. Distrib.* **2014**, *8*, 1007–1016. [CrossRef]
22. Watanabe, S.; Kinoshita, M.; Hosokawa, T.; Morigaki, K.; Nakura, K. Capacity fade of $LiAl_yNi_{1-x-y}Co_xO_2$ cathode for lithium-ion batteries during accelerated calendar and cycle life tests (surface analysis of $LiAl_yNi_{1-x-y}CoxO_2$ cathode after cycle tests in restricted depth of discharge ranges). *J. Power Sources* **2014**, *258*, 210–217. [CrossRef]
23. Vetter, J.; Novák, P.; Wagner, M.; Veit, C.; Möller, K.C.; Besenhard, J.; Winter, M.; Wohlfahrt-Mehrens, M.; Vogler, C.; Hammouche, A. Ageing mechanisms in lithium-ion batteries. *J. Power Sources* **2005**, *147*, 269–281. [CrossRef]
24. Laresgoiti, I.; Käbitz, S.; Ecker, M.; Sauer, D.U. Modeling mechanical degradation in lithium ion batteries during cycling: Solid electrolyte interphase fracture. *J. Power Sources* **2015**, *300*, 112–122. [CrossRef]
25. Wang, J.; Liu, P.; Hicks-Garner, J.; Sherman, E.; Soukiazian, S.; Verbrugge, M.; Tataria, H.; Musser, J.; Finamore, P. Cycle-life model for graphite-LiFePO4 cells. *J. Power Sources* **2011**, *196*, 3942–3948. [CrossRef]
26. Millner, A. Modeling lithium ion battery degradation in electric vehicles. In *Proceedings of the 2010 IEEE Conference on Innovative Technologies for an Efficient and Reliable Electricity Supply*; IEEE: Piscataway, NJ, USA, 2010; pp. 349–356.
27. Kassem, M.; Bernard, J.; Revel, R.; Pelissier, S.; Duclaud, F.; Delacourt, C. Calendar aging of a graphite/LiFePO4 cell. *J. Power Sources* **2012**, *208*, 296–305. [CrossRef]
28. Apribowo, C.H.B.; Sarjiya, S.; Hadi, S.P.; Wijaya, F.D. Optimal planning of battery energy storage systems by considering battery degradation due to ambient temperature: A review, challenges, and new perspective. *Batteries* **2022**, *8*, 290. [CrossRef]
29. Xu, B.; Zhao, J.; Zheng, T.; Litvinov, E.; Kirschen, D.S. Factoring the Cycle Aging Cost of Batteries Participating in Electricity Markets. *IEEE Trans. Power Syst.* **2018**, *33*, 2248–2259. [CrossRef]
30. Lee, Y.R.; Kim, H.J.; Kim, M.K. Optimal operation scheduling considering cycle aging of battery energy storage systems on stochastic unit commitments in microgrids. *Energies* **2021**, *14*, 470. [CrossRef]
31. Lee, J.O.; Kim, Y.S. Novel battery degradation cost formulation for optimal scheduling of battery energy storage systems. *Int. J. Electr. Power Energy Syst.* **2022**, *137*, 107795. [CrossRef]
32. Liu, C.; Ma, H.; Zhang, H.; Shi, X.; Shi, F. A MILP-based battery degradation model for economic scheduling of power system. *IEEE Trans. Sustain. Energy* **2022**, *14*, 1000–1009. [CrossRef]
33. Saxena, S.; Roman, D.; Robu, V.; Flynn, D.; Pecht, M. Battery stress factor ranking for accelerated degradation test planning using machine learning. *Energies* **2021**, *14*, 723. [CrossRef]
34. Nebuloni, R.; Ilea, V.; Berizzi, A.; Bovo, C.; Meraldi, L.; Moretti, L.; Raboni, P. A MILP Battery Degradation Logarithmic Model with Real-Time Cycle Counting Calculation. *IEEE Trans. Ind. Appl.* **2025**, *61*, 8297–8306. [CrossRef]

Disclaimer/Publisher's Note: The statements, opinions and data contained in all publications are solely those of the individual author(s) and contributor(s) and not of MDPI and/or the editor(s). MDPI and/or the editor(s) disclaim responsibility for any injury to people or property resulting from any ideas, methods, instructions or products referred to in the content.